Journal of Magnetism and Magnetic Materials 322 (2010) 530–535

Contents lists available at ScienceDirect

Journal of Magnetism and Magnetic Materials

journal homepage: www.elsevier.com/locate/jmmm

Spin wave spectrum of magnetic nanotubes

A.L. González [a], P. Landeros [b,*], Álvaro S. Núñez [a]

[a] Departamento de Física, Facultad de Ciencias Físicas y Matemáticas, Universidad de Chile, Casilla 487-3, Santiago, Chile
[b] Departamento de Física, Universidad Tĕcnica Federico Santa María, Avenida España 1680, Valparaíso 2340000, Chile

ARTICLE INFO

Article history:
Received 15 August 2009
Available online 8 October 2009

PACS:
75.10.−b
75.30.Ds
75.60.Ch
75.75.+a

Keywords:
Nanomagnetism
Spin wave
Magnetic nanotube
Ferromagnetism
Domain wall
Vortex

ABSTRACT

We investigate the spin wave spectra associated to a vortex domain wall confined within a ferromagnetic nanotube. Basing our study upon a simple model for the energy functional we obtain the dispersion relation, the density of states and dissipation induced life-times of the spin wave excitations in presence of a magnetic domain wall. Our aim is to capture the basics spin wave physics behind the geometrical confinement of nobel magnetic textures.

1. Introduction

In the last years, the synthesis of magnetic nanotubes (MNs) have triggered a new and broad research field, encompassing both their physical properties and their possible applications in different areas. Although their magnetic properties are slightly different than, and potentially advantageous over the ones for ferromagnetic nanowires, magnetic tubes have been poorly explored in spite that they exhibits core-free magnetic configurations, leading to more controllable reversal process, ensuring reproducibility and efficiency. MNs are object of current research interest not only for the understanding of their basic properties, also because they exhibit potential applications in nano and biotechnology [1,2].

From the experimental standpoint there are some methods for the fabrication of MNs, as hydrogen reduction [3], electrodeposition [4] and atomic layer deposition [5] into porous membranes. There are also some fundamental works involved to the knowledge of basic magnetic properties, as the internal magnetic structure [6–10], nucleation phenomena [10–13], reversal process [14,15], domain wall (DW) motion [16] and spin waves [6,17,18]. It has been argued that the reversal process occurs via nucleation and propagation of DWs, which may be a transverse wall for tube radius (R) smaller than a critical radius ($R_c(\beta)$), or a vortex wall for $R > R_c(\beta)$ [14]. This critical radius depends on the magnetic material and on a shape factor defined as $\beta \equiv R_i/R$, with R_i the internal radius of the nanotube. The critical radius ranges from a few nm to 20 nm approximately, and then, since MNs currently fabricated have $R > R_c(\beta)$, we can expect that the nucleation and propagation of a vortex DW be the dominant magnetization reversal mechanism for MNs [14].

Elementary excitations in magnetism has been investigated over decades [19,20] and still being an active and important issue, mainly because the reduced dimensionality has dramatic consequences in the magnetic behavior, as one can see in the phenomenology that magnetic thin films presents [19,20]. More recently, it has been reported that a DW confined within a ferromagnetic nanostrip can interact with a SW [21–25]. The authors argued that a SW change their phase as they pass through a magnetic DW [21,22]. Besides, DWs in magnetic nanostripes can be manipulated and set in motion via interaction with SWs [23]. According to the theory presented by Le Maho et al. [24], current-driven DWs might be viewed as the generators of SWs. Besides, in the case of 2D ferromagnets, Wieser et al. [25] have reported the existence of SW modes bound inside a DW. Clearly, for the prospective technological implementation of devices including or manipulating DWs or SWs, the interplay between these magnetic entities has to necessarily be understood. The above mentioned interesting characteristics of SWs and DWs motivate us to perform this study in the nanotube topology. We are interested

* Corresponding author.
E-mail address: pedro.landeros@usm.cl (P. Landeros).

0304-8853/$ - see front matter © 2009 Elsevier B.V. All rights reserved.
doi:10.1016/j.jmmm.2009.10.010

here in the case that there is a vortex DW within the MN. The paper is organized as follows: in Section 2 we present the theoretical background, Section 3 is devoted to the SW excitations, whereas in Section 4 we discuss the role of Gilbert damping. Our main results and conclusions are summarized in Section 5.

2. Theoretical background

In this section we describe the evolution of the magnetization $\mathbf{M}(\mathbf{r};t)=M_s\mathbf{m}(\mathbf{r};t)$ in a MN with a vortex DW. The main assumption used in this work is the ideal cylindrical shape of the nanotubes, which simplifies in great manner the calculations. To characterize the evolution of $\mathbf{M}$ we use the formalism of the Landau–Lifshitz–Gilbert (LLG) equation [26] in a suitable form. Then the dispersion relation for the SW and the eigen-modes of oscillation for the precessing spins can be obtained. Since the field dynamics we are describing conserve the norm of $\mathbf{M}$, we can use angular variables Θ and Φ to describe the orientation of the spins as follows:

$$m_\rho=\sin\Theta(\phi,z)\cos\Psi(\phi,z), \tag{1}$$

$$m_\phi=\sin\Theta(\phi,z)\sin\Psi(\phi,z), \tag{2}$$

$$m_z=\cos\Theta(\phi,z). \tag{3}$$

Since we focus our interest in MNs with a small thickness, we have assumed that our variables does not depend on the radial coordinate.

Landau–Lifshitz equations can be stated for Θ and Ψ in the usual way. However we find it more convenient write them in terms of canonical variables $\mathcal{P}=\Psi$ and $\mathcal{Q}=\cos\Theta$. Written in those variables, the dissipation-free Landau–Lifshitz equation is casted in an explicit Hamiltonian representation. Naturally, an associated action principle can be created in terms of an action functional whose minima are solutions of the dissipation-free LL equation. This action can be written as

$$S=\int \mathrm{d}t\,\mathrm{d}^3r\left(\mathcal{P}\dot{\mathcal{Q}}-\frac{\gamma}{M_s}\varepsilon[\mathbf{M}]\right), \tag{4}$$

where γ is the gyromagnetic ratio and M_s the saturation magnetization. The dynamical equations obtained from Eq. (4), gives the evolution for Θ and Ψ, hence the dynamics of the spin system. Stationary magnetization textures are static minima of this action. We shall calculate the quadratic fluctuations around such solutions and identify them as spin-wave excitations. The main task, to which everything is reduced, is the search of an accurate expression for the energy functional $\varepsilon[\mathbf{M}]$ and compute the dynamical equations, this is done in the following sections.

2.1. Basic assumptions and the energy model

First of all, we work under the assumption that the tubes are confined within ideal cylindrical shapes. Also we assume that their length L is much bigger than any other relevant length-scale of the problem. Usual parameters are in the order of $R\sim 15-300\,\mathrm{nm}$, $\beta\sim 0.8-0.95$ and $L\sim 1-30\,\mu\mathrm{m}$ [4,5].

We adopt a continuous description of the system defined by the magnetization $\mathbf{M}(\mathbf{r};t)$. The total magnetic energy is composed by four contributions [26,27], that is $\varepsilon[\mathbf{M}]=\varepsilon_x+\varepsilon_d+\varepsilon_Z+\varepsilon_K$ where $\varepsilon_x=A\int\sum(\nabla m_i)^2\,\mathrm{d}v$ is the exchange energy, with $m_i=M_i/M_s$ $(i=x,y,z)$ the cartesian components of the magnetization normalized to the saturation value M_s, and A the stiffness constant. The dipolar contribution is written as $\varepsilon_d=(\mu_0/2)\int\mathbf{M}\cdot\nabla U\,\mathrm{d}v$, with U the magnetostatic potential, whereas ε_Z is the Zeeman term. The last contribution ε_K comes from anisotropy. Depending on the sample preparation and experimental details, the anisotropy contribution can be either a magnetocrystalline anisotropy (cubic or uniaxial), or a spin–orbit based surface anisotropy, or both. Surface anisotropy can be influential in the precise results, and this contribution can be easily included within our theory. However, since we lack experimental information on the role of surface anisotropy in MNs we regard the quantitative tuning that could be achieved with its inclusion as inappropriate at this stage. Therefore, we neglect surface anisotropy in our calculations. We also take advantage of the geometry of the MN neglecting the volumetric term of the dipolar energy due to the negligible thickness of the tube. Also the dipolar surface energy is captured by an anisotropy like term. This shape anisotropy is modeled by a sum of infinitesimal capacitors with charge proportional to the local magnetic charge. For the capacitors we assume that the field lines are closed very tightly from the inner surface toward to the outer one. After these considerations and setting aside the external field contribution, the energy can be cast in the form:

$$\varepsilon[\mathbf{M}]=\int\mathrm{d}v\left[A\sum(\nabla m_i)^2-K(\hat{\mathbf{z}}\cdot\mathbf{m})^2\right]+\frac{As}{2\pi\ell^2}\int\mathrm{d}z\,\mathrm{d}\phi(\hat{\boldsymbol{\rho}}\cdot\mathbf{m})^2, \tag{5}$$

where $s=\pi R^2(1-\beta^2)$ is the tube cross section, K the uniaxial anisotropy constant and $\ell\equiv\sqrt{2A/\mu_0M_s^2}$ stands for the exchange length of the given material. We are now in position to calculate the explicit form of the terms involved in the energy functional. By using the expressions for the magnetization field, the energy functional can be expressed as

$$\varepsilon[\Theta,\Psi]=\frac{sA}{2\pi}\int\mathcal{E}[\Theta,\Psi]\,\mathrm{d}z\,\mathrm{d}\phi, \tag{6}$$

where

$$\mathcal{E}=(\partial_z\Theta)^2+\frac{1}{b^2}(\partial_\phi\Theta)^2 -\frac{1}{W^2}\cos^2\Theta+\left\{(\partial_z\Psi)^2+\frac{1}{\ell^2}\cos^2\Psi+\frac{1}{b^2}(1+\partial_\phi\Psi)^2\right\}\sin^2\Theta. \tag{7}$$

Here we have defined $1/b^2\equiv 2\pi\log(1/\beta)/s$, whereas $W\equiv\sqrt{A/K}$ stands for the width of a DW due to the interplay of the exchange and uniaxial anisotropy energies in a bulk sample.

2.2. Linearization of the equations of motion

With the above energy functional in hand, we can find the equilibrium states or investigate the SW normal modes as well. To do this we need to expand the magnetization around a minimal energy configuration, which is achieved by doing $\Theta\to\Theta_0(z,\phi)+\overline{\Theta}(z,\phi)$ and $\Psi\to\Psi_0(z,\phi)+\overline{\Psi}(z,\phi)$, where $\Theta_0(z,\phi)$ and $\Psi_0(z,\phi)$ stands for the minimal energy configuration. The zeroth order correction in the energy functional does not contribute with anything new, whereas the first order correction give us the minimum of the energy functional. Thus, we can write the energy functional as $\varepsilon[\Theta,\Psi]=sA/2\pi\int\{\mathcal{E}^{(0)}+\mathcal{E}^{(1)}+\mathcal{E}^{(2)}+\cdots\}\,\mathrm{d}z\,\mathrm{d}\phi$, where $\mathcal{E}^{\{i\}}$ is the i-th order contribution. The first order contribution can be written as $\mathcal{E}^{(1)}=\mathcal{E}^{(1)}_{\mathrm{ex}}+\mathcal{E}^{(1)}_{\mathrm{ani}}$, where $\mathcal{E}^{(1)}_{\mathrm{ex}}$ and $\mathcal{E}^{(1)}_{\mathrm{ani}}$ are displayed in Appendix A. One of the solutions of the associated Euler equation is a vortex wall [14–16] given by

$$\cos\Theta_0=\tanh(z/\lambda),\quad \Psi_0=\pi/2, \tag{8}$$

where $1/\lambda^2=1/b^2+1/W^2$ is a measure of the DW width and was obtained from energy minimization. From this point onward we shall use this width as the basic unit of length. As mentioned earlier, depending on the geometrical parameters, the MN will support different types of DWs [14,16]. In the case of vortex DWs the magnetization goes from pointing upwards to downward, through a vortex-like structure. In the center of the wall (at $z=z_0$), the magnetization wraps around the cylinder with vanishing

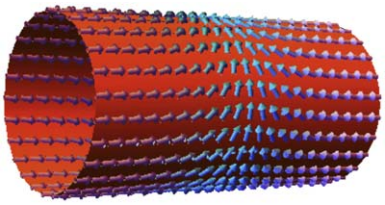

Fig. 1. Illustration of a vortex domain wall confined in a ferromagnetic nanotube.

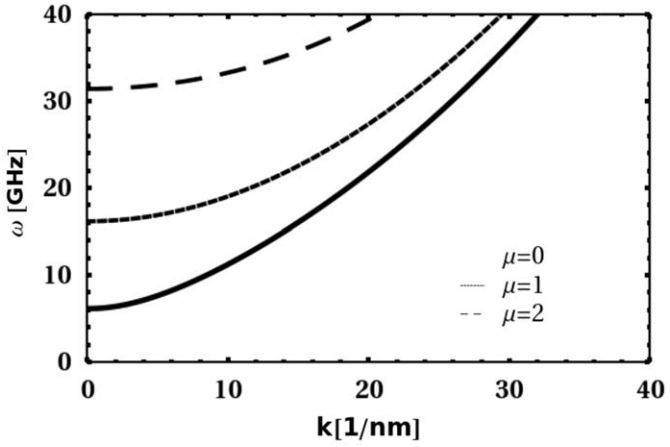

Fig. 2. Plot of the dispersion relation for the mode without transversal excitations, $\mu=0$. MN parameters are: $R=25$ nm, $\beta=0.9$, and $\ell=\lambda/10$.

component along the z axis. Note that a static vortex wall in a MN does not have any radial component of the magnetization, avoiding the creation of magnetic charges at the tube cylindrical surfaces, and then reducing the magnetostatic energy. On the other hand the curling of the magnetization increments the exchange energy, which is increased if the tube radius is small enough, and the resultant DW structure is a transverse DW [14,16]. Recent calculations show that for MNs with radius bigger than a few exchange lengths, the energetically favorable structure is a vortex DW [14,16], as the reader can see schematically in Fig. 1.

From the second order term in the energy functional we can investigate the SW normal modes of the system. Their dynamics could be analyzed considering or not the magnetic DW.

3. Spin wave excitations

In this section we will obtain the SW spectra associated to a vortex DW confined within an infinite nanotube. Our aim is to capture the basics physics behind the geometrical confinement of nobel magnetic textures, as the vortex wall. This can be done by inspection of the second order term of the energy functional, which can be written as, $\mathcal{E}^{(2)}=\mathcal{E}^{(2)}_{\rm ex}+\mathcal{E}^{(2)}_{\rm ani}$, where $\mathcal{E}^{(2)}_{\rm ex}$ and $\mathcal{E}^{(2)}_{\rm ani}$ are displayed in Appendix A. As long as we restrict the fields to be small in magnitude we can write the Fourier expansion:

$$\overline{\Theta}=\sum_{\mu}\overline{\Theta}_{\mu}(z)e^{i\mu\phi}, \tag{9}$$

and the respective expression for $\overline{\Psi}$. The integration over the variable ϕ clearly reduces the energy into a sum of uncoupled $\mu-$modes:

$$\mathcal{E}^{(2)}=\sum_{\mu}\mathcal{E}^{(2)}_{\mu}, \tag{10}$$

where the expression for $\mathcal{E}^{(2)}_{\mu}$ is displayed in Appendix A. For each $\mu-$mode the dynamical contribution (or Berry phase) to the action is given by

$$\mathcal{P}\dot{\mathcal{Q}}=\sum_{\mu}\overline{\Theta}_{\mu}\dot{\Psi}^{*}_{\mu}. \tag{11}$$

Away from the DW, large fluctuations of the angle Ψ become irrelevant, since the actual physical field $\mathbf{m}(\mathbf{r})$ does not change along with them. This, of course, correspond to the well known singularity of the polar coordinates representation and does not represent any intrinsic feature of the physics at hand. The actual physical variable, however, can naturally be isolated through the change of variables:

$$\Lambda_{\mu}=\Psi_{\mu}\sin\Theta_0, \tag{12}$$

that will be used from this point onward. The equation of motion for the SWs reads

$$-\dot{\Lambda}_{\mu}=\mathcal{L}_{\mu}\overline{\Theta}_{\mu}-2i\mu(\lambda^2/b^2)\tanh(z)\overline{\Lambda}_{\mu}, \tag{13}$$

$$\dot{\Theta}_{\mu}=(\mathcal{L}_{\mu}-\lambda^2/\ell^2)\overline{\Lambda}_{\mu}+2i\mu(\lambda^2/b^2)\tanh(z)\overline{\Theta}_{\mu}, \tag{14}$$

where we have made:

$$\mathcal{L}_{\mu}=\partial_z^2-\mu^2\lambda^2/b^2-1+2\mathrm{sech}^2 z. \tag{15}$$

In these equations and in the following manipulations we have chosen λ as the basic unit of length and $1/\tau\equiv\gamma A/M_s\lambda^2$ as the unit of time. Our main task of characterizing the SWs of a MN reduces now to solve the eigen-problem given by Eqs. (13) and (14). A special note is deserved by the rather interesting close analogy between the resulting equations and the well known time dependent Bogoliubov or Bogoliubov–de Gennes equations [28].

3.1. Exact solution for $\mu=0$

The special case $\mu=0$, correspond essentially to a 1D-system and admits an straightforward solution, along the same lines of Refs. [29,30]. The equation is simply:

$$\begin{pmatrix}-\dot{\Lambda}\\ \dot{\Theta}\end{pmatrix}=\begin{pmatrix}0 & \mathcal{L}_0\\ \mathcal{L}_0-d^2 & 0\end{pmatrix}\begin{pmatrix}\Lambda\\ \Theta\end{pmatrix}, \tag{16}$$

in which $\mathcal{L}_0=\partial_z^2-1+2\mathrm{sech}^2 z$ and $d^2\equiv\lambda^2/\ell^2$. If Λ and Θ are chosen to be eigenfunctions of $\mathcal{L}_0$ with eigenvalue $-\sigma$, it follows that:

$$\ddot{\Theta}=-\sigma(\sigma+d^2)\Theta, \tag{17}$$

$$\ddot{\Lambda}=-\sigma(\sigma+d^2)\Lambda. \tag{18}$$

To obtain the eigenvalues and eigenvectors of $\mathcal{L}_0$ we recognize the form of a Schrödinger equation with a Pöschl–Teller type potential with a specific selection of parameters. This kind of equations has been observed recently by Wieser et al. [25] for one dimensional systems with a transverse DW. We note, however that, for this specific set of parameters, bound states localized around the DW structure are not allowed. The diagonalization of such system can be found in standard text of elementary quantum mechanics [31] in terms of associated Legendre polynomials. After some elementary manipulations, the SW eigenstates are given by

$$\Lambda_k(z)=\frac{1}{\sqrt{2\pi(1+k^2)}}e^{ikz}(-ik+\tanh z), \tag{19}$$

where the dimensionless wave vector has been normalized to $1/\lambda$. The dispersion relation $\omega(k)$ is obtained by substituting $\Lambda=\Lambda(z)e^{-i\omega t}$ in Eq. (18),

$$\omega^2_{wall}=(k^2+1)(k^2+1+(\lambda/\ell)^2). \tag{20}$$

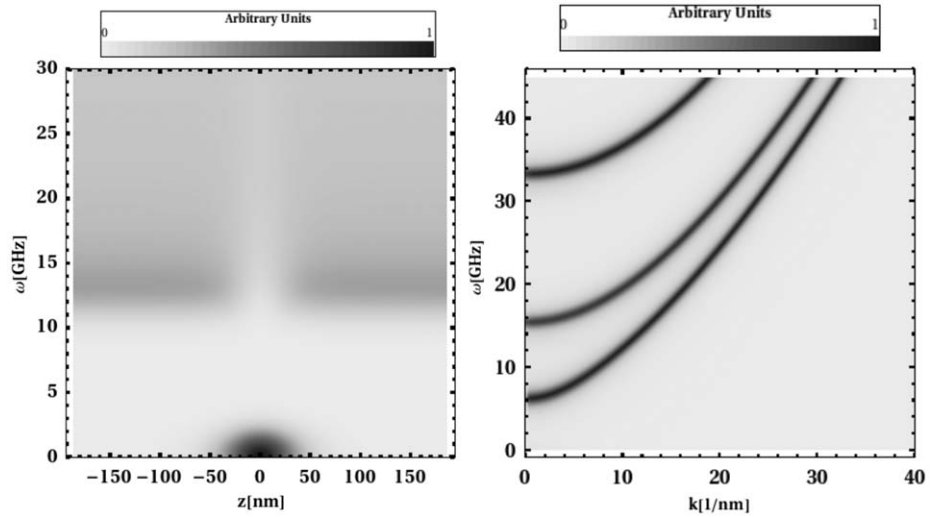

Fig. 3. The left panel depicts the SW energy spectrum (Eq. (25)) showing the local energy density as a function of the frequency of the mode. Notice that the vortex DW is located at the center of the tube (at $z=0$). The right panel shows the power density spectrum, defined in the text through Eq. (24). It correspond to the momentum representation of the eigen-mode.

Now from Eq. (16) the relation between Λ and Θ is established:

$$\Theta = -i\frac{\omega_{wall}}{\sigma}\Lambda = i\sqrt{\frac{k^2+1+(\lambda/\ell)^2}{k^2+1}}\Lambda. \tag{21}$$

Eqs. (19) and (21) fully determine the behavior of the axially symmetric spin-wave excitations. From them we can clearly recognize a k-dependent phase shift of the spin-wave modes as they pass across the domain wall, in agreement with recent articles [21,22,25]. The value of the phase shift ϕ_k is given by $\tan\phi_k = 2k/(k^2-1)$.

3.2. Solutions in the general case $\mu \neq 0$

Now we look back into Eqs. (13) and (14) and found the general dispersion relation for $\mu > 0$. To do this, we take the asymptotic limit ($z\to\infty$), and we obtain

$$\begin{pmatrix} -\dot{\Lambda} \\ \dot{\Theta} \end{pmatrix} = \begin{pmatrix} -2i\mu\dfrac{\lambda^2}{b^2} & -\mathcal{L}_\mu^{(\infty)} \\ \mathcal{L}_\mu^{(\infty)} - \dfrac{\lambda^2}{\ell^2} & 2i\mu\dfrac{\lambda^2}{b^2} \end{pmatrix} \begin{pmatrix} \Lambda \\ \Theta \end{pmatrix}, \tag{22}$$

where $\mathcal{L}_\mu^{(\infty)} = \partial_z^2 - \mu^2\lambda^2/b^2 - 1$. The last equation can be easily diagonalized, finding the following dispersion relation,

$$\omega^2 = \left(k^2+1+\mu^2\frac{\lambda^2}{b^2}\right)\left(k^2+1+\mu^2\frac{\lambda^2}{b^2}+\frac{\lambda^2}{\ell^2}\right)+4\mu^2\frac{\lambda^4}{b^4}. \tag{23}$$

We remark that if we take the limit ($z\to-\infty$), the same results are obtained. Naturally by using $\mu=0$ in Eq. (23), the expression (20) is regained.

The task of finding the eigenmodes of the SW spectrum cannot be done analytically, and then we resort on a numerical approach. For each μ−mode we solve Eqs. (13) and (14) with the harmonic time dependence. This is simply an eigenvalue equation that in the discretized version can be solved by diagonalizing a matrix. We label the different eigenvalues with the index σ. The eigen-frequencies are then labeled by $\omega_{\mu\sigma}$, and the eigen-modes by the pair $\Theta_{\mu\sigma}(z)$ and $\Lambda_{\mu\sigma}(z)$. To identify a momentum dependence of the eigenvalues we perform a numerical Fourier transform.

To summarize the main results of our calculations we present two distinct plots for the power density spectrum and the energy

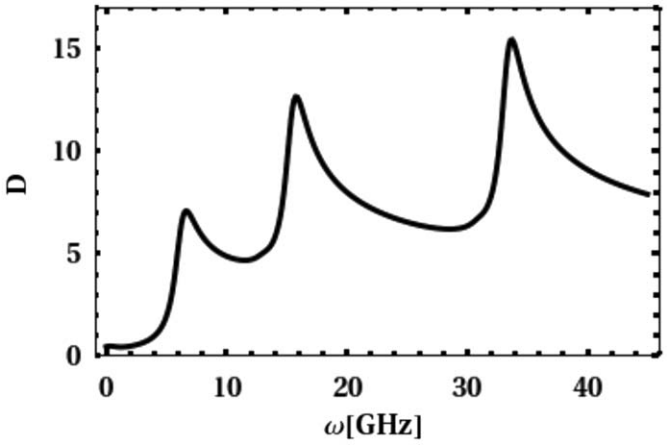

Fig. 4. Net SW density of states showing the aggregated spectrum along the momentum axis. The plots are based on the case with $R=25$ nm, $\beta=0.9$, and $\ell=\lambda/10$. Note the relation of the branches here calculated and the ones of Fig. 2.

density spectrum. The first can be defined as

$$\rho(k,\omega) = \sum_{\mu\sigma}\delta(\omega-\omega_{\mu\sigma})(|\Theta_{\mu\sigma}(k)|^2+|\Lambda_{\mu\sigma}(k)|^2), \tag{24}$$

while the energy density spectrum is defined as

$$\rho_E(z,\omega) = \sum_{\mu\sigma}\delta(\omega-\omega_{\mu\sigma})\mathcal{E}_{\mu\sigma}(z). \tag{25}$$

The density spectra just defined, along with the density of states $D(\omega)=\sum_k\rho(k,\omega)$, are displayed in Figs. 3 and 4, respectively.

4. Effects of Gilbert damping

To account for damping effects we must leave the simple action principle provided by Eq. (4). The action still is given by Eq. (4) but must be complemented by a dissipative function [32], that in the case of the LLG phenomenology is

$$\mathcal{R} = \frac{\alpha}{2}\int \mathrm{d}t\,\mathrm{d}^3x\left(\frac{\dot{\mathcal{Q}}^2}{1-\mathcal{Q}^2}+(1-\mathcal{Q}^2)\dot{\mathcal{P}}^2\right). \tag{26}$$

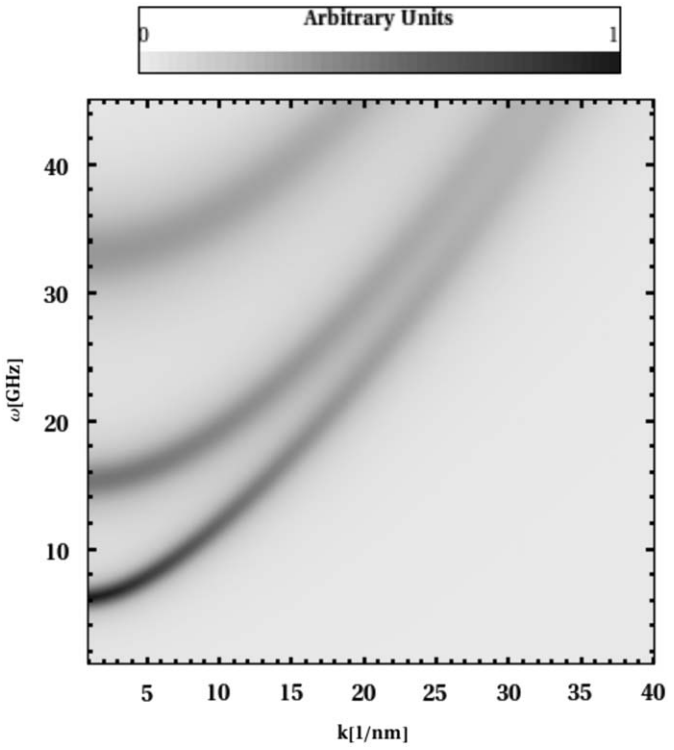

Fig. 5. Power density spectrum, defined in the text through Eq. (24). It correspond to the momentum representation of the eigen-mode. The plots are based on the case with $\alpha=0.1$, $R=25\,\mathrm{nm}$, $\beta=0.9$ and $\ell=\lambda/10$. Note the relation of the branches here calculated and the ones of Fig. 2. The thickness of the branches is related to the life-time of the excitations.

The equations of motion can be cast in the form:

$$\frac{\delta\mathcal{S}}{\delta\mathcal{Q}}=\frac{\delta\mathcal{R}}{\delta\dot{\mathcal{Q}}}\quad\text{and}\quad\frac{\delta\mathcal{S}}{\delta\mathcal{P}}=\frac{\delta\mathcal{R}}{\delta\dot{\mathcal{P}}}. \tag{27}$$

For the sake of simplicity we will focus the discussion again in the simpler case of $\mu=0$. The analysis is completely analogous in the case of $\mu\neq 0$, but the algebra is more involved. The only effect of the Gilbert damping is the addition of a dissipation term to the equations, which now take the form:

$$\begin{pmatrix}-\dot{\Sigma}\\ \dot{\Theta}\end{pmatrix}=\begin{pmatrix}0 & \mathcal{L}_0\\ \mathcal{L}_0-d^2 & 0\end{pmatrix}\begin{pmatrix}\Sigma\\ \Theta\end{pmatrix}+\begin{pmatrix}0 & \alpha\\ \alpha & 0\end{pmatrix}\begin{pmatrix}\dot{\Sigma}\\ \dot{\Theta}\end{pmatrix}. \tag{28}$$

Following the path of previous sections, we look for solutions in terms of eigenstates of $\mathcal{L}_0$ and we obtain:

$$\begin{pmatrix}i\omega & (k^2+1+i\alpha\omega)\\ (k^2+1+d^2+i\alpha\omega) & -i\omega\end{pmatrix}\begin{pmatrix}\Sigma\\ \Theta\end{pmatrix}=0. \tag{29}$$

This equation can be easily diagonalized and the resulting dispersion relation can be expressed as:

$$(\alpha^2+1)\omega=\sqrt{(k^2+1)(d^2+k^2+1)-d^4\alpha^2/4}+i\alpha(d^2/2+k^2+1). \tag{30}$$

Clearly, by setting $\alpha=0$ the above dispersion relation (see Eq. (20)) is regained. The complex term in the frequency accounts for the energy dissipation, manifesting itself in the form of a life-time for the spin-waves.

The calculation for the case of $\mu\neq 0$ goes along the same lines. We start by numerically diagonalizing the discrete version of the problem and then display the frequency–momentum dependence. We restrict ourselves just to show the final results summarized in the power density spectrum shown in Fig. 5. The width of the lines here convey the information of the life-time for each mode.

5. Final remarks

In this paper we have work out the spin wave spectrum of isolated ferromagnetic nanotubes supporting vortex domain wall configurations. By taking advantage of the reduced thickness of the tubes we can reliably simplify the field degrees of freedom to those on the cylindrical shell. The cylindrical geometry of those systems provides a natural way to partially diagonalize the SW system in to several quasi-one dimensional subsystems labeled by the axial angle dependence mode. We have derived the small amplitude SW spectrum as a function of the reduced 1D wave vector. Two effects are the main results of the interplay of the SWs and the magnetic DW. First, SWs are scattered by the DW, and this scattering results in phase shifts associated with SWs moving to and from the domain wall. The other result is the increment of the band gap for spin waves. This effect is related to the higher energy associated with perturbing a DW. Our results are based in the exact solution of the linearized Landau–Lifshitz–Gilbert equation.

Acknowledgments

It is with great pleasure that the authors thank Alejandro Jara and Prof. Rodrigo Arias for useful discussions. This work was partially funded by Proyecto de Iniciación en investigación FONDECYT, through grants 11070008 and 11080246, Millennium Science Nucleus "Basic and Applied Magnetism" P06-022-F, and the program "Bicentenario en Ciencia y Tecnología" PBCT under projects PSD-031 and ACT027.

Appendix A

In what follows we show explicitly the first and second order terms in the expansion of the energy functional. The first order exchange term can be cast in the form:

$$\begin{aligned}\mathcal{E}^{(1)}_{\mathrm{ex}}&=2(\partial_z\Theta_0)(\partial_z\overline{\Theta})+(2/b^2)(\partial_\phi\Theta_0)(\partial_\phi\overline{\Theta})\\&\quad+\{(\partial_z\Psi_0)^2+(1/b^2)(1+\partial_\phi\Psi_0)^2\}\overline{\Theta}\sin(2\Theta_0)\\&\quad+2(\partial_z\Psi_0)(\partial_z\overline{\Psi})+(2/b^2)(1+\partial_\phi\Psi_0)(\partial_\phi\overline{\Psi}),\end{aligned} \tag{31}$$

while the first order anisotropy term reduces to

$$\begin{aligned}\mathcal{E}^{(1)}_{\mathrm{ani}}&=(1/W^2+\cos^2(\Psi_0)/\ell^2)\overline{\Theta}\sin(2\Theta_0)\\&\quad-(1/\ell^2)\overline{\Psi}\sin(2\Psi_0)\sin\Theta_0.\end{aligned} \tag{32}$$

The corresponding second order terms are given by

$$\begin{aligned}\mathcal{E}^{(2)}_{\mathrm{ex}}&=(sA/\pi)\{(\partial_z\overline{\Theta})^2+\sin^2\Theta_0(\partial_z\overline{\Psi})^2\}\\&\quad+(sA/\pi b^2)\{(\partial_\phi\overline{\Theta})^2+\cos(2\Theta_0)\overline{\Theta}^2\\&\quad+\sin^2\Theta_0(\partial_\phi\overline{\Psi})^2+2\sin(2\Theta_0)\overline{\Theta}\partial_\phi\overline{\Psi}\},\end{aligned} \tag{33}$$

and

$$\mathcal{E}^{(2)}_{\mathrm{ani}}=\cos(2\Theta_0)\overline{\Theta}^2/W^2-\sin^2\Theta_0\overline{\Psi}^2/\ell^2. \tag{34}$$

Finally, the term $\mathcal{E}^{(2)}_{\mu}$ in Eq. (10) is given by

$$\begin{aligned}\frac{\mathcal{E}^{(2)}_{\mu}}{2sA}&=|\partial_z\overline{\Theta}_\mu|^2+\sin^2\Theta_0|\partial_z\overline{\Psi}_\mu|^2\\&\quad+(1/b^2)\{\mu^2|\overline{\Theta}_\mu|^2+\cos(2\Theta_0)|\overline{\Theta}_\mu|^2\\&\quad+\sin^2(\Theta_0)\mu^2|\overline{\Psi}_\mu|^2+2i\sin(2\Theta_0)\overline{\Theta}_\mu\Psi^*_\mu\}\\&\quad+\cos(2\Theta_0)|\overline{\Theta}_\mu|^2/W^2-\sin^2\Theta_0|\overline{\Psi}_\mu|^2/\ell^2.\end{aligned} \tag{35}$$

References

[1] S.J. Son, J. Reichel, B. He, M. Schuchman, S.B. Lee, J. Am. Chem. Soc. 127 (2005) 7316–7317.
[2] D. Lee, R.E. Cohen, M.F. Rubner, Langmuir 23 (2007) 123.
[3] Y.C. Sui, R. Skomski, K.D. Sorge, D.J. Sellmyer, J. Appl. Phys. 95 (2004) 7151.
[4] K. Nielsch, F.J. Castaño, C.A. Ross, R. Krishnan, J. Appl. Phys. 98 (2005) 034318; K. Nielsch, F.J. Castaño, S. Matthias, W. Lee, C.A. Ross, Adv. Eng. Mater. 7 (2005) 217.
[5] M. Daub, M. Knez, U. Gösele, K. Nielsch, J. Appl. Phys. 101 (2007) 09J111.
[6] Z.K. Wang, H.S. Lim, H.Y. Liu, S.C. Ng, M.H. Kuok, L.L. Tay, D.J. Lockwood, M.G. Cottam, K.L. Hobbs, P.R. Larson, J.C. Keay, G.D. Lian, M.B. Johnson, Phys. Rev. Lett. 94 (2005) 137208.
[7] J. Escrig, P. Landeros, D. Altbir, E.E. Vogel, P. Vargas, J. Magn. Magn. Mater. 308 (2007) 233–237.
[8] J. Lee, D. Suess, T. Schrefl, K. Hwan Oh, J. Fidler, J. Magn. Magn. Mater. 310 (2007) 2445–2447.
[9] A.P. Chen, N.A. Usov, J.M. Blanco, J. Gonzalez, J. Magn. Magn. Mater. 316 (2007) e317–e319.
[10] P. Landeros, O.J. Suarez, A. Cuchillo, P. Vargas, Phys. Rev. B 79 (2009) 024404.
[11] C.R. Chang, C.M. Lee, J.S. Yang, Phys. Rev. B 50 (1994) 6461.
[12] J. Escrig, M. Daub, P. Landeros, K. Nielsch, D. Altbir, Nanotechnology 18 (2007) 445706.
[13] N.A. Usov, A.P. Chen, A. Zhukov, J. Gonzalez, J. Appl. Phys. 104 (2008) 083902.
[14] P. Landeros, S. Allende, J. Escrig, E. Salcedo, D. Altbir, E.E. Vogel, Appl. Phys. Lett. 90 (2007) 102501.
[15] N.A. Usov, A. Zhukov, J. Gonzalez, J. Magn. Magn. Mater. 316 (2007) 255–261.
[16] P. Landeros, A.S. Núñez, Domain wall motion on ferromagnetic nanotubes, submitted.
[17] H. Leblond, V. Veerakumar, Phys. Rev. B 70 (2004) 134413.
[18] T.M. Nguyen, M.G. Cottam, Surface Sci. 600 (2006) 4151–4154.
[19] M.G. Cottam, Linear and Nonlinear Spin Waves in Magnetic Films and Superlattices, World Scientific, Singapore, 1994.
[20] S.O. Demokritov, B. Hillebrands, Spin waves in laterally confined magnetic structures, in: B. Hillebrands, K. Ounadjela (Eds.), Spin Dynamics in Confined Magnetic Structures, vol. I, Springer, Berlin, Heidelberg, 2002.
[21] R. Hertel, W. Wulfhekel, J. Kirschner, Phys. Rev. Lett. 93 (2004) 257202.
[22] C. Bayer, H. Schultheiss, B. Hillebrands, R.L. Stamps, IEEE Trans. Magn. 41 (2005) 3094.
[23] D.S. Han, S.K. Kim, J.Y. Lee, S.J. Hermsdoerfer, H. Schultheiss, B. Leven, B. Hillebrands, Appl. Phys. Lett. 94 (2009) 112502.
[24] Y.L. Maho, J.V. Kim, G. Tatara, Phys. Rev. B 79 (2009) 174404.
[25] R. Wieser, E.Y. Vedmedenko, R. Wiesendanger, Phys. Rev. B 79 (2009) 144412.
[26] A. Aharoni, Introduction to the Theory of Ferromagnetism, Clarendon Press, Oxford, 1996.
[27] J. Stöhr, H.C. Stiegmann, Magnetism, From Fundamentals to Nanoscale Dynamics, Springer, Berlin Heidelberg, 2006.
[28] J.B. Ketterson, S.N. Song, Superconductivity, Cambridge University Press, New York, 1999.
[29] J.M. Winter, Phys. Rev. 124 (1961) 452.
[30] A.A. Thiele, Phys. Rev. B 7 (1973) 391.
[31] L.D. Landau, E.M. Lifshitz, Quantum Mechanics (Vol. 3 of Course of Theoretical Physics), third ed., Butterworth-Heinemann, 1981.
[32] L.D. Landau, E.M. Lifshitz, Mechanics (Vol. 1 of Course of Theoretical Physics), third ed., Butterworth-Heinemann, 1982.